

## Experimental demonstration of a left-handed metamaterial operating at 100 GHz

M. Gokkavas,<sup>1,\*</sup> K. Guven,<sup>1,2</sup> I. Bulu,<sup>1,2</sup> K. Aydin,<sup>1,2</sup> R. S. Penciu,<sup>4</sup> M. Kafesaki,<sup>4</sup> C. M. Soukoulis,<sup>4,5</sup> and E. Ozbay<sup>1,2,3</sup>

<sup>1</sup>Nanotechnology Research Center, Bilkent University, Bilkent, 06800 Ankara, Turkey

<sup>2</sup>Department of Physics, Bilkent University, Bilkent, 06800 Ankara, Turkey

<sup>3</sup>Department of Electrical and Electronics Engineering, Bilkent University, Bilkent, 06800 Ankara, Turkey

<sup>4</sup>Institute of Electronic Structure and Laser, Foundation for Research and Technology, Hellas and Department of Materials Science and Technology, University of Crete, Greece

<sup>5</sup>Ames Laboratory-USDOE and Department of Physics and Astronomy, Iowa State University, Ames, Iowa 50011, USA

(Received 22 March 2006; published 12 May 2006)

The existence of a left-handed (LH) transmission band in a bulk composite metamaterial (CMM) around 100 GHz is demonstrated experimentally. The CMM consists of stacked planar glass layers on which periodic patterns of micron-scale metallic wires and split-ring resonators are fabricated. The LH nature of the CMM band is proved by comparing the transmission spectra of individual CMM components. Theoretical investigation of the CMM by transmission simulations and an inversion scheme for the retrieval of the effective permeability and permittivity functions supports the existence of LH behavior.

DOI: [10.1103/PhysRevB.73.193103](https://doi.org/10.1103/PhysRevB.73.193103)

PACS number(s): 42.70.-a, 41.20.Jb, 78.20.Ci, 81.05.Zx

The idea of left-handed (LH) materials, i.e., materials with both negative electrical permittivity ( $\epsilon$ ) and magnetic permeability ( $\mu$ ), where the electric field ( $\mathbf{E}$ ), magnetic field ( $\mathbf{B}$ ), and wave vector ( $\mathbf{k}$ ) form a left-handed coordinate system, was developed by Veselago<sup>1</sup> decades ago. It was only recently that such materials were realized in a composite metamaterial (CMM) form consisting of stacked planar  $\epsilon < 0$  and  $\mu < 0$  components.<sup>2,3</sup> The electromagnetic phenomena and the potential applications<sup>4</sup> (e.g., the formation of a perfect lens<sup>5</sup>) associated with these materials have quickly evolved into a solid research field. While obtaining the  $\epsilon < 0$  response was relatively easy (e.g., using wire arrays<sup>6</sup>), the realization of  $\mu < 0$  response beyond MHz range has been a challenge, due to the absence of naturally occurring magnetic materials. Pendry *et al.* suggested a design made of concentric metallic rings with gaps, called split ring resonators (SRRs) which exhibit  $\mu < 0$  response in the vicinity of a certain magnetic resonance frequency  $\omega_m$ .<sup>7</sup> The  $\omega_m$  depends essentially on the geometrical parameters of the SRR structure, and it can be tuned virtually from MHz to THz range by straightforward scaling of these parameters. Based on these two fundamental components, different CMM designs are reported.<sup>2,3,8</sup>

The fabrication of CMMs for infrared and optical regime necessitates higher resolution photolithography as well as thinner substrates, or even the use of a single substrate coupled with multilayer processing. Up to date, the highest resonance frequency from SRR type structures is reported to be 100 THz; the relevant medium was e-beam patterned SRRs on a single substrate layer, and the resonance was induced through coupling to the electric field, where an excitation with  $\mathbf{k}$  perpendicular to the SRRs-plane is used.<sup>9</sup> This monolayer approach<sup>9,10</sup> works fine, since the periodicity of SRRs in the direction perpendicular to their plane is not essential for the resonance. The multilayer SRR-only medium with a THz magnetic resonance reported up to date was obtained by a multilayer microfabrication process, in which a few layers of two-dimensional (2D)-SRR arrays separated by

polyimide coating were fabricated on a single substrate.<sup>11</sup> However, for the demonstration of LH behavior (i.e., both  $\epsilon < 0$  and  $\mu < 0$  response) in a CMM, where the periodicity in the stacking direction is crucial, the multilayer-single-substrate technology is extremely difficult to implement, since one needs many layers (to achieve a thickness comparable to the operation wavelength). Recently, Moser *et al.* reported a transmission peak at 2.5 THz from a CMM-type material measured by Fourier transform infrared spectroscopy.<sup>12</sup> Their results were obtained from a monolayer of in-plane SRR and wire arrays under normal incidence. Although this was a proof of concept for one layer CMM, the lack of multi-layer CMM structure prevented the demonstration of true LH behavior. This demonstration is possible only when the magnetic resonance is excited by the magnetic field (as opposed to excitation by the electric field such as in Ref. 12), which requires a  $\mathbf{k}$  component parallel to the SRR-wire planes (so that the SRRs respond as a  $\mu < 0$  material<sup>13</sup>). Another recent study employs planar arrays of pairs of metal nanorods which is a promising CMM design aiming the THz regime.<sup>14</sup>

We stress that the THz-structure<sup>13</sup> shows only  $\mu < 0$  and not yet a negative refractive index,  $n$ . In this letter, we report the experimental realization of a bulk multilayer-CMM, which exhibits a LH transmission peak at 100 GHz with  $n < 0$ . While the scalability is the key principle to project an available design to different operation frequencies in a straightforward manner, we would like to elucidate the point that a refined approach is needed for the practical realization which is subject to available material and fabrication constraints. For instance, at  $f \sim 100$  GHz, typical metals (e.g., Cu, Au) have a skin depth,  $\delta$ , of  $\sim 0.25 \mu\text{m}$  which may imply a lower threshold for the deposition thickness with proper metallic behavior. This, in turn, brings the problem of fabricating the metamaterial features with acceptable uniformity (in particular the gap regions between the rings and the splits of SRRs). The uniformity of the gap regions is critical since they determine the resonance frequency of the structure. Lack of simple but precise formulas for determining the

resonance frequency of SRRs necessitates the use of intensive numerical calculations. The dielectric substrate generates a nonuniform distribution of the local field of SRRs,<sup>18</sup> which then affects the capacitive-inductive (LC) resonance of the SRR; hence, the substrate brings an additional constraint for the design. We used standard 22 mm  $\times$  22 mm  $\times$  150  $\mu\text{m}$  layers of Corning glass as the substrate. This thickness ensures structural rigidity and the air gap between the layers present in the microwave structures is eliminated.

An essential part of the design is the wire-only medium with a plasma frequency  $\omega_p$ , high above the  $\omega_m$  of SRRs. The actual  $\omega_p$  of the CMM is lower than that of its wire-only component, due to the additional electric response of SRRs.<sup>8,15</sup> Hence, one has to ensure that the  $\omega_p$  of the CMM (i.e., the edge of the  $\epsilon < 0$  stop band) remains above  $\omega_m$  (i.e.,  $\mu < 0$  region) for the existence of a LH transmission band. This, in turn, requires a high  $\omega_p$  of wire-only medium to start with. We employ the formulation by Pendry *et al.* for the  $\omega_p$  in metallic mesostructures which relates the microscopic quantities (effective electron density,  $n_{\text{eff}}$ , and electron mass,  $m_{\text{eff}}$ ) to the macroscopic parameters of the system (wire radius,  $r$  and the periodicity of the lattice,  $a$ ),

$$\omega_p^2 = \frac{n_{\text{eff}} e^2}{\epsilon_0 m_{\text{eff}}} = \frac{2\pi c_0^2}{a^2 \ln(ar)}. \quad (1)$$

This expression provides a clear description of the physics of the plasmon in terms of the design parameters of the structure. At fixed periodicity, the only possibility for higher  $\omega_p$  appears to be the enlargement of  $r$ . Yet, this yields only a marginal increase factor of  $\omega_p'/\omega_p = [\ln(r/a)/\ln(r'/a)]^{1/2}$ , where  $r, r' < a/2$  since in this case both  $n_{\text{eff}}$  and  $m_{\text{eff}}$  acquires an enhancement. Instead, we employ a design in which the unit cell accommodates multiple wires. In this case,  $m_{\text{eff}}$  would roughly be the same (since the wire radius did not change) but  $n_{\text{eff}}$  is multiplied by  $M$ , the number of wires. In addition, multiple wire pattern results in less absorption for the transmitting signal compared to that of the single thick wire designed for the same  $\omega_p$ .

Figures 1(a) and 1(b) show one unit cell of the SRR and the wire micro-patterns, respectively. The unit cell of the CMM contains one SRR, and two layers of triple wire pattern. Employing two consecutive wire layers increases the coupling and the overall density of wires, which shifts  $\omega_p$  further higher. The dimensions of the components are as follows: Inner ring inner radius:  $r_{ii}=43 \mu\text{m}$ , inner ring outer radius:  $r_{io}=67.2 \mu\text{m}$ , outer ring inner radius:  $r_{oi}=80.7 \mu\text{m}$ , outer ring outer radius:  $r_{oo}=107.5 \mu\text{m}$ , split ring gap:  $d=7.2 \mu\text{m}$ , wire width:  $w=26.9 \mu\text{m}$ , wire separation:  $d_w=53.7 \mu\text{m}$ . The periodicity in  $x$ - and  $y$ -directions is  $a_x=a_y=262.7 \mu\text{m}$ .

The metamaterial patterns are printed on glass substrates by employing UV-photolithography followed by microfabrication with a metal thickness of 100  $\text{\AA}$  Ti/4500  $\text{\AA}$  Au. For SRR-only and wire-only structures, plain glass layers (denoted as “glass” in the figures below) were used as spacers, so that the resulting periodicity is the same as in the CMM structure. All structures have 10 unit cells in the propagation direction. The CMM was composed of 100 layers, having a

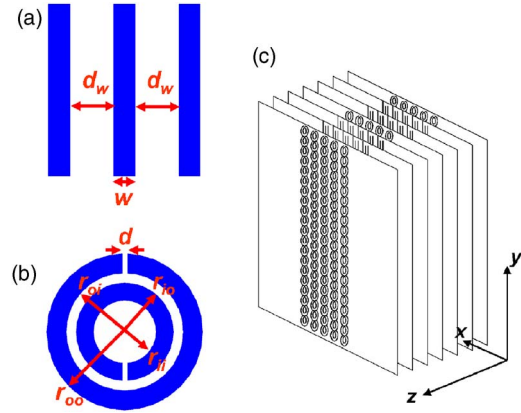


FIG. 1. (Color online) (a) Wire and (b) SRR geometry employed for the CMM. (c) Schematic of the CMM, consisting of periodically stacked (along  $z$ ) two layers of wire-patterned substrates and one layer of SRR-patterned substrate. The propagation direction for the electromagnetic field is along the  $x$  axis.

15 mm (100  $\times$  150  $\mu\text{m}$ ) width ( $z$ ), 20 mm height ( $y$ ), and 2.6 mm length ( $x$ ),  $x$  being the propagation direction. Figure 1(c) shows the schematic of the CMM, while Fig. 2 is a photomicrograph of one SRR-layer and stacked on top of one wire-layer. The patterns were aligned to the substrate edge during photolithography, thus, the alignment within the resulting metamaterial is limited by the edge uniformity of the substrate layers.

The transmission spectrum was measured by a millimeter wave network analyzer. Figure 3 shows the normal-to-the-plane transmission spectrum of SRR-only for two different SRR orientations. In this configuration, the resonance of SRR can be excited only through the electric field,<sup>13</sup> when the SRR is asymmetric with respect to  $E$  (lower three curves). Since the asymmetric orientation causes a misbalance of the charge distribution and induces circulating currents on SRRs, the result is a resonant electric response of the system, which appears as a gap. On the other hand, the

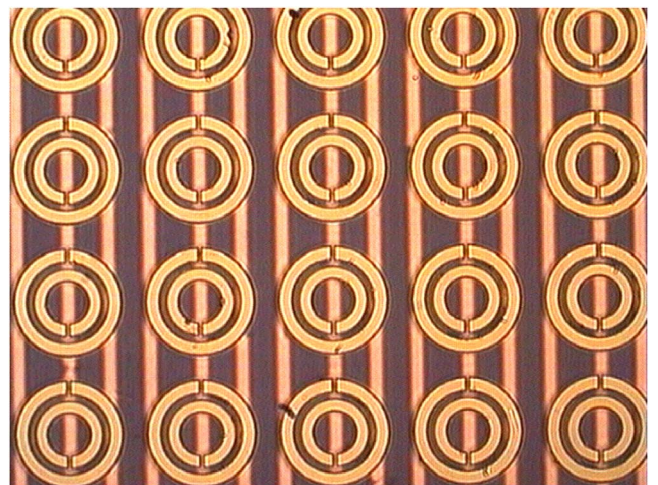


FIG. 2. (Color online) Photomicrograph showing the CMM sample. The SRR (front) and wire (back) layers were aligned by the edges of the glass substrates.

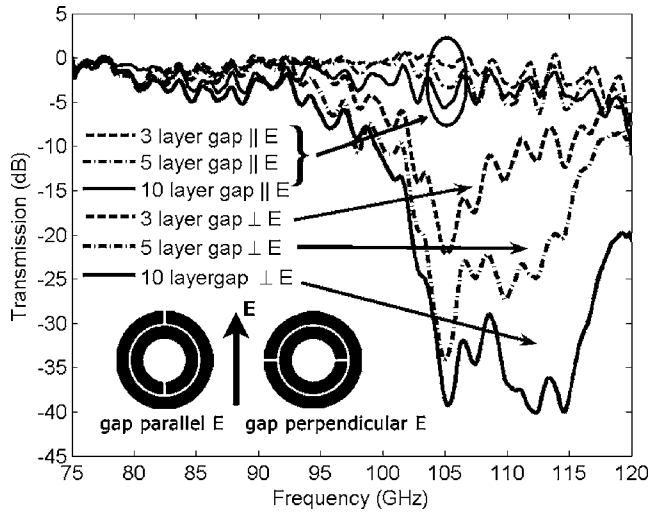


FIG. 3. Transmission spectra of the SRR-only structure for propagation normal to the SRR plane for different number of layers along the propagation direction with SRR-splits parallel (upper three curves, marked in circle) and perpendicular (lower three curves) to the electric field vector  $E$ . The resonant behaviour occurs in the latter case.

symmetric orientation with respect to  $E$  (upper three curves, marked in circle) is transparent. Increasing the number of layers enhances and, due to interlayer coupling between SRRs, widens the resonance gap. In order to avoid electric coupling, we employ the symmetric orientation in the CMM.

Figure 4 shows the transmission spectra of wire-only, SRR-only, and closed ring resonator (CRR)-only structures. The CRR is just the SRR with splits closed, and thus has no magnetic response. The legend denotes the components in one unit cell. The  $\epsilon < 0$  stop-band of the wire-only structure spans the measured frequency range. The onset of transmission above 120 GHz signals the  $\omega_p$  of wires. The SRR-only

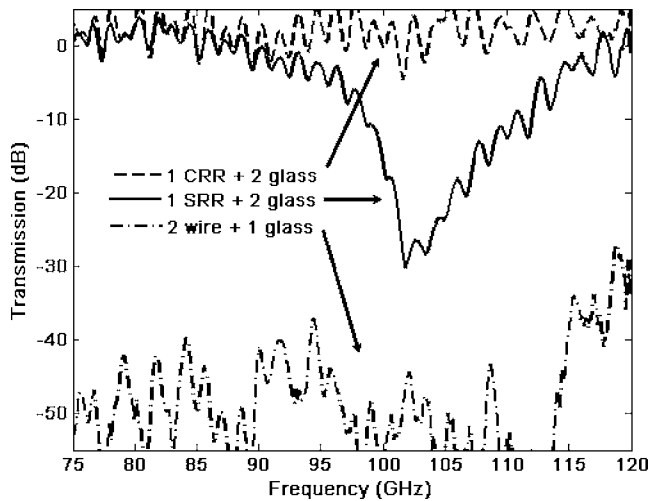


FIG. 4. Transmission spectra of CRR only (dashed line), SRR only (solid line), and wire only (dash-dotted line) structures. The legend denotes the respective number of layers within one unit cell of the assembled structure. “Glass” is a plain glass substrate layer used as spacer.

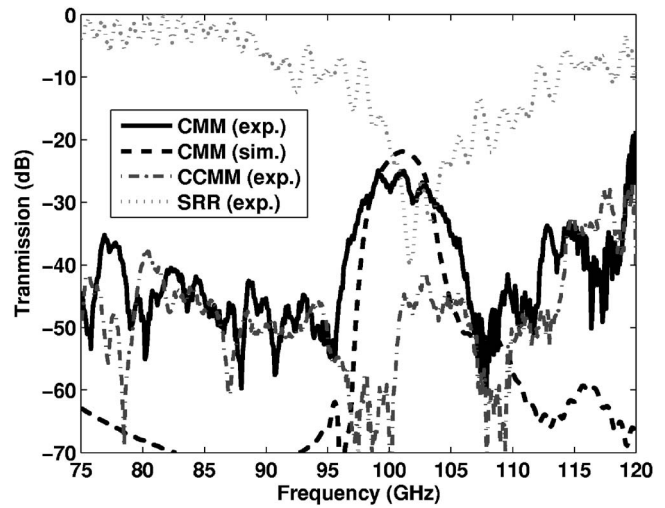


FIG. 5. The experimental (solid black line) and simulated (dashed black line) transmission spectra of CMM. At around 100 GHz, the  $\mu < 0$  gap of the SRR-only structures (dotted light gray line) matches the transmission band of the CMM. In contrast, the transmission spectra of the CCMM (dash-dotted gray line) is opaque in this range. The increase of the transmission at 120 GHz signals the onset of a right-handed transmission band (plasma cut-off frequency) for the CMM and CCMM.

structure exhibits a resonance ( $\mu < 0$ ) between 95 and 108 GHz with  $-30$  dB minimum occurring at 102 GHz whereas the CRR-only medium is transparent, as expected.

In order to contrast the CMM response, a “nonworking” CMM is made by replacing SRR layers with CRR layers (called CCMM here).<sup>8</sup> Figure 5 shows the measured transmission spectra of CMM structures incorporating SRRs (black solid line), and CRRs [blue (gray) solid line], respectively. The simulated CMM transmission (dashed black line) will be discussed further below. The CMM structure exhibits a clear pass band between 96 and 107 GHz with a  $-25$  dB

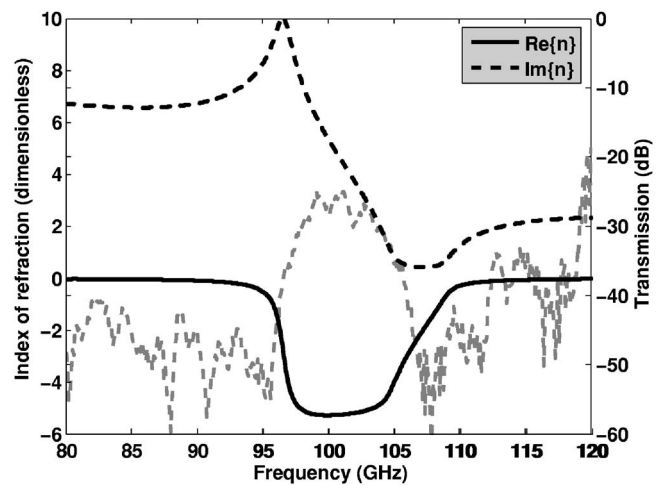


FIG. 6. (Left axis) The real (solid black) and imaginary (dashed black) parts of the frequency dependent index of refraction computed by retrieval procedure. (Right axis) The dotted light gray line shows the measured transmission band of the CMM for comparison.

maximum at 101 GHz. We stress that this band matches the  $\mu < 0$  stop band of SRRs (shown by the light gray dotted line). On the other hand, the CCMM [blue (gray) solid line] remains opaque, because it is essentially a  $\varepsilon < 0$  medium.

The simulations are done by a commercial software (MICROWAVE STUDIO) which employs the finite integration technique for solving Maxwell's equations. Two main assumptions apply to the simulated structure: (i) The loss of metal and substrate are included by reference conductance values, and the finite thickness of the metal (in relation to skin depth) is not considered. (ii) Disorder is not included. As reported in a recent study,<sup>17</sup> fabrication-based nonuniformity of SRR and wire elements (especially close to the mask edges), and misalignment induced by variations in substrate size are inherent problems, which may degrade the transmission significantly. Nevertheless, the theoretical transmission spectrum for the CMM plotted in Fig. 5 shows good agreement with the experimental results. The calculated  $\omega_p$  for the wire-only structure is above 150 GHz; therefore, the wire spectrum is not shown. Figure 6 shows the refractive index,  $n$ , of the CMM computed through the retrieval procedure<sup>16</sup> relative to the measured transmission spectra of a single layer CMM. The real part of  $n(f)$  is negative within the

transmission band of the CMM with a value of  $-5.2$  at  $f = 100$  GHz.

In conclusion, we have demonstrated the left-handed behavior in the multilayer SRR+wire type CMM at 100 GHz. The operation frequency is one order of magnitude above the previously reported values. The CMM was fabricated on glass-substrates, using photolithography, and microfabrication. The transmission band of the CMM was located well within the  $\varepsilon < 0$  stop-band of the structure, coincided with the  $\mu < 0$  stop-band of the SRR-only medium, and disappeared when the splits of the SRRs were shorted, proving unambiguously its left-handed nature. The experimental results are strongly supported by the theoretical simulations.

#### ACKNOWLEDGMENTS

This work was supported by the projects EU-DALHM, EU-NOE-METAMORPHOSE, EU-NOE-PHOREMOST, TUBITAK-104E090, DARPA-HR0011-05-C-0068, and Greek Ministry of Education PYTHAGORAS and by Ames Laboratory (Contract No. W-7405-Eng-82). E.O. acknowledges partial support from the Turkish Academy of Sciences. The research of C.M.S. is further supported by the Alexander von Humboldt senior-scientist award 2002.

\*Corresponding author. Electronic address:  
mgokkavas@fen.bilkent.edu.tr

<sup>1</sup>V. G. Veselago, *Sov. Phys. Usp.* **10**, 504 (1968).

<sup>2</sup>D. R. Smith, W. J. Padilla, D. C. Vier, S. C. Nemat-Nasser, and S. Schultz, *Phys. Rev. Lett.* **84**, 4184 (2000).

<sup>3</sup>R. A. Shelby, D. R. Smith, S. C. Nemat-Nasser, and S. Schultz, *Appl. Phys. Lett.* **78**, 480 (2001).

<sup>4</sup>N. Engheta and R. W. Ziolkowski, *IEEE Trans. Microwave Theory Tech.* **53**, 1535 (2005).

<sup>5</sup>J. B. Pendry, *Phys. Rev. Lett.* **85**, 3966 (2000).

<sup>6</sup>J. B. Pendry, A. J. Holden, W. J. Stewart, and I. Youngs, *Phys. Rev. Lett.* **76**, 4773 (1996).

<sup>7</sup>J. B. Pendry, A. J. Holden, D. J. Robbins, and W. J. Stewart, *IEEE Trans. Microwave Theory Tech.* **47**, 2075 (1999).

<sup>8</sup>K. Aydin, K. Guven, M. Kafesaki, L. Zhang, C. M. Soukoulis, and E. Ozbay, *Opt. Lett.* **29**, 2623 (2004).

<sup>9</sup>S. Linden, C. Enkrich, M. Wegener, J. Zhou, T. Koschny, and C. M. Soukoulis, *Science* **306**, 1351 (2004).

<sup>10</sup>T. J. Yen, W. J. Padilla, N. Fang, D. C. Vier, D. R. Smith, J. B. Pendry, D. N. Basov, and X. Zhang, *Science* **303**, 1494 (2004).

<sup>11</sup>N. Katsarakis, G. Konstantinidis, A. Kostopoulos, R. S. Penciu, T. F. Gundogdu, M. Kafesaki, E. N. Economou, T. Koschny, and C. M. Soukoulis, *Opt. Lett.* **30**, 1348 (2005).

<sup>12</sup>H. O. Moser, B. D. F. Casse, O. Wilhelmi, and B. T. Saw, *Phys. Rev. Lett.* **94**, 063901 (2005).

<sup>13</sup>N. Katsarakis, T. Koschny, M. Kafesaki, E. N. Economou, and C. M. Soukoulis, *Appl. Phys. Lett.* **84**, 2943 (2004).

<sup>14</sup>V. M. Shalaev, W. Cai, U. K. Chettiar, Hsiao-Kuan Yuan, A. K. Sarychev, V. P. Drachev, and A. V. Kildishev, *Opt. Lett.* **30**, 3356 (2005).

<sup>15</sup>T. Koschny, M. Kafesaki, E. N. Economou, and C. M. Soukoulis, *Phys. Rev. Lett.* **93**, 107402 (2004).

<sup>16</sup>D. R. Smith, D. C. Vier, T. Koschny, and C. M. Soukoulis, *Phys. Rev. E* **71**, 036617 (2005).

<sup>17</sup>K. Aydin, K. Guven, N. Katsarakis, C. M. Soukoulis, and E. Ozbay, *Opt. Express* **12**, 5896 (2004).

<sup>18</sup>M. Kafesaki, T. Koschny, R. S. Penciu, T. F. Gundogdu, E. N. Economou, and C. M. Soukoulis, *J. Opt. A, Pure Appl. Opt.* **7**, S12 (2005).